Gümüşhane University Journal of Science and Technology

GUFBD / *GUJS* (2026) 16(4): 1117-1128 doi: 10.17714/gumusfenbil.1924998 Research Article

Interaction between strontium sulfate and boric acid at high temperatures in the presence of activated charcoal

İlhan EHSANİ[1], Arman EHSANİ[2], Ayşe ÜÇYILDIZ[3], Raşit SEZER[4], Abdullah OBUT*[3]

[1]*Şırnak University, Engineering Faculty, Mining Engineering Department, 73000, Şırnak*

[2]*Adana Alparslan Türkeş Science and Technology University, Engineering Faculty, Mining Engineering Department, 01250, Adana*

[3]*Hacettepe University, Engineering Faculty, Mining Engineering Department, 06800, Ankara*

[4]*Karadeniz Technical University, Engineering Faculty, Metallurgical and Materials Engineering Department, 61040, Trabzon*

• Received: 07.04.2026 • Accepted: 07.10.2026

Abstract

In this study, the interaction between strontium sulfate ($SrSO_4$) and boric acid (H_3BO_3), both in the absence and presence of activated charcoal (C), was investigated at high temperatures using an $SrSO_4$:H_3BO_3 molar ratio of 1:2, which corresponds to the stoichiometric composition of strontium metaborate (SrB_2O_4). It was found that in the absence of C, $SrSO_4$ and H_3BO_3 did not interact to form SrB_2O_4 upon heating at either 1073 K and 1273 K, probably due to the very high thermal stability of $SrSO_4$. In contrast, in the presence of C, heating at 1073 K resulted in the formation of minor amounts of strontium borate phases, such as SrB_6O_{10} and SrB_4O_7, whereas the SrB_2O_4 phase was formed upon heating at 1273 K. The formation of SrB_2O_4 was further confirmed by Fourier transform infrared spectroscopy analysis. Furthermore, when reagent-grade $SrSO_4$ was replaced with natural $SrSO_4$ (celestine) in the starting mixture containing H_3BO_3 and C, the formation of SrB_2O_4 was also achieved at 1273 K. Because of the promising results obtained for strontium metaborate, this study should be extended for the preparation other strontium and alkaline earth metal (i.e., Ca) borates from corresponding naturally abundant sulfates that are usually not preferred as the starting compounds in high-temperature solid-state synthesis studies.

Keywords: Activated Charcoal, Boric Acid, Celestine, Strontium metaborate, Strontium sulfate

1. Introduction

There are approximately 153 strontium-containing minerals found in the Earth's crust (IMA, 2022). Among them, celestine (natural $SrSO_4$) is the most commonly mined strontium mineral and is used as the primary strontium source following the production of concentrates with grades over 90-92% $SrSO_4$ from its ores using different beneficiation (i.e. gravity concentration or flotation) techniques (Griffiths, 1992; Hong, 1993).

Celestine has limited use and is almost always converted to strontium carbonate ($SrCO_3$), which is the most important industrial strontium compound, by using two different extractive metallurgical processes; namely the black ash and the direct conversion (also known as the double decomposition) processes. In the former process, celestine is reacted firstly with carbon (in the form of coal, petroleum coke, or metallurgical grade coke) at temperatures ≥1273 K to produce water-soluble strontium sulfide, SrS, as the intermediate compound. Then, the produced solid sulfide is dissolved in hot water, undissolved residue is separated from the loaded solution and finally, strontium is precipitated from the solution as $SrCO_3$ using either sodium carbonate or carbon dioxide as the precipitating agent. In the latter process, celestine is interacted with hot sodium carbonate solution directly to produce $SrCO_3$. If the quality of produced strontium carbonate is low, it is leached with acid and re-precipitated again to obtain a higher quality product (Griffiths, 1992; Hong, 1993; Sezer et al., 2020).

The anhydrous binary SrO-B_2O_3 system, which includes different stoichiometric compounds, such as SrB_4O_7, SrB_2O_4, $Sr_2B_2O_5$, etc., has attracted attention due to the various optical properties exhibited by different strontium borates. The orthorhombic SrB_2O_4 (strontium metaborate) compound, which melts congruently at 1431 K (Pan et al., 2004), is one of the stoichiometric members of the SrO-B_2O_3 system and may be used as a

*Abdullah OBUT; aobut@hacettepe.edu.tr

light-emitting phosphor after doping with rare earth ions, i.e. green-emitting with Tb^{3+} (Wu et al., 2012) or blue-emitting with Eu^{2+} (Zheng et al., 2015), as a non-flammable, anti-corrosive, anti-bacterial and/or anti-fungal pigment (Ohtsu et al., 1994) and as a nanomaterial (Li et al., 2011).

Until now, various procedures, i.e. high-temperature solid-state synthesis method (Rulmont & Almou, 1989; Onodera et al., 1999; Berezovskaya et al., 2007; Wu et al., 2012; Zhao et al., 2012; Zheng et al., 2015; Zhang et al., 2016; Zheng et al., 2020), solution combustion method (Pekgözlü & Karabulut, 2009; Gawande et al., 2014), the sol-gel method followed by calcination (Li et al., 2011), micro-pulling down method with radio frequency heating (Fujimoto et al., 2011), Pechini method (Runowski et al., 2018) etc., were used for the preparation of SrB_2O_4. Among them, the high-temperature solid-state synthesis method, generally applied at temperatures ≥1073 K using $SrCO_3$-H_3BO_3 or $SrCO_3$-B_2O_3 starting mixtures, is the most studied one.

Although naturally occurring strontium sulfate, celestine, is the most common and cheapest strontium source, it is not preferred as the starting strontium source in the preparation of inorganic strontium compounds due to its very high thermal and chemical stabilities. Therefore, in this study, for the first time in the literature, the interaction between strontium sulfate and boric acid at high temperatures was investigated using mainly X-ray diffraction analyses to reveal the possible formation conditions of strontium metaborate in the absence and presence of activated charcoal, which can convert strontium sulfate into more reactive strontium sulfide phase.

2. Materials and Methods

2.1. Materials

In the experimental studies, strontium sulfate ($SrSO_4$, Carlo Erba), strontium sulfide (SrS, Alfa Aesar), boric acid (H_3BO_3, PanReac), and activated charcoal (C, Merck) were used. In addition, diboron trioxide (B_2O_3, min. 98%, Eti Mine) and natural strontium sulfate (mineral 'celestine', >98% $SrSO_4$) were also used in some experiments for comparison purposes.

The starting mixtures; namely, $SrSO_4$-H_3BO_3 (S-B), $SrSO_4$-activated charcoal (S-C), $SrSO_4$-H_3BO_3-activated charcoal (S-B-C), celestine-activated charcoal (Cel-C), celestine-H_3BO_3-activated charcoal (Cel-B-C), and SrS-B_2O_3 (SS-BO) mixtures; were prepared by hand-mixing the above-mentioned initial reactants in a mortar. The S-B, S-B-C, and Cel-B-C mixtures were prepared considering the stoichiometry of SrB_2O_4, i.e. for 1 mole of Sr, 2 moles of B were used. The amount of activated charcoal used in the preparation of the S-C, S-B-C, and Cel-B-C mixtures was selected considering the formation of SrS according to Equation (1), i.e. for 1 mole of $SrSO_4$, 4 moles of C were used. For the SS-BO mixture, 1 mol Sr containing SrS was interacted with 2 mol B containing B_2O_3.

$$SrSO_4 + 4C \rightarrow SrS + 4CO \quad (1)$$

2.2. Methods

The mixtures that contained activated charcoal were heated in porcelain crucibles (Isolab) covered with porcelain lids, and those that did not contain activated charcoal were heated in open porcelain crucibles. Each crucible was heated separately in a muffle furnace (Nüve) at a heating rate of 10 K/60 s starting from room temperature to the set temperature, which was selected according to the preliminary experiments and the literature studies (Chen & Zhu, 2000; Sonawane et al., 2000; Liu & Huang, 2006; Abdel Halim et al., 2009; Erdemoğlu, 2009; Setoudeh et al., 2011) as 1073 K and 1273 K. After being kept at the set temperature for 3600 s, the heating was stopped, and the furnace was left to cool to room temperature. After completing the heating-cooling sequence, the obtained samples were pulverized in a mortar by hand and their X-ray diffraction (XRD) patterns (Rigaku, CuKα radiation) were determined.

Because of the inevitable presence of gaseous oxygen (in air) during heat-treatment in the muffle furnace, some of the selected activated charcoal-containing mixtures were also subjected to heat treatment in a tube furnace (MTI GSL-1100X) under an inert atmosphere of argon. The mixtures were heated in alumina boats from room temperature to 1273 K at a heating rate of 10 K/60 s under high-purity (99.999%) Ar flow. After holding at 1273 K for 3600 s, the furnace was allowed to cool naturally to room temperature under the same

inert atmosphere. Upon completion of the heating-cooling cycle, the resulting products were hand-ground in a mortar, and their XRD patterns (PANalytical, CuKα radiation) were determined using a diffractometer.

The thermal analyses (TG/DTA curves) of $SrSO_4$, H_3BO_3, and the S-B mixture were performed using a thermal analyzer (Setaram) under static air atmosphere at heating rate of 10 K/60 s. The thermal behaviours of activated charcoal-containing, the S-C and the S-B-C, mixtures were determined by using a thermal analyzer (Netzsch) under inert (Ar) atmosphere at heating rate of 10 K/60 s.

The Fourier transform infrared-attenuated total reflection (FTIR-ATR) spectra and the morphologies of selected heated mixtures were also determined using a spectrometer (Thermo Fisher) and scanning electron microscope (SEM) equipments (FEI and TESCAN GAIA3).

3. Results and discussion

In the first place, the TG/DTA curves of $SrSO_4$ and H_3BO_3 were determined separately (Figure 1), and it was observed that they were in good agreement with the corresponding curves reported in the previous literature studies (Kauffman & Dilling, 1950; Hatakeyama & Liu, 1998; Sevim et al., 2006; Üçyıldız, 2008; Aghili et al., 2018). Then, the interaction between $SrSO_4$ and H_3BO_3 (the S-B mixture) was investigated, considering the possible formation of SrB_2O_4 in a direct manner. For this purpose, the TG/DTA curves (Figure 2) of the S-B mixture were first determined. As shown in Figure 2, H_3BO_3 in the initial mixture decomposes with increasing temperature in accordance with Equation (2) (see also Figure 1), and is present in the mixture in the form of B_2O_3 at both 1073 K and 1273 K. As also seen in Figure 2, no thermal events, endothermic or exothermic, were observed in the DTA curve of the S-B mixture between 1073 K and 1273 K, indicating that no synthesis reactions or interactions occurred between $SrSO_4$ and B_2O_3.

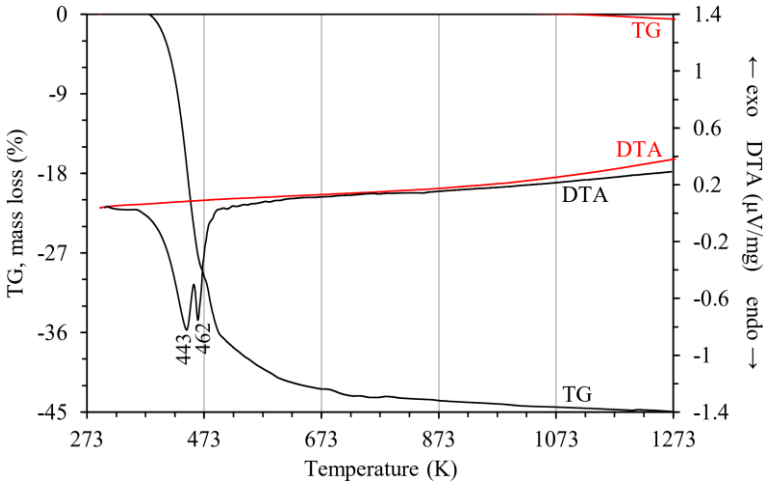


Figure 1. TG/DTA curves of $SrSO_4$ (red) and H_3BO_3 (black) under air atmosphere

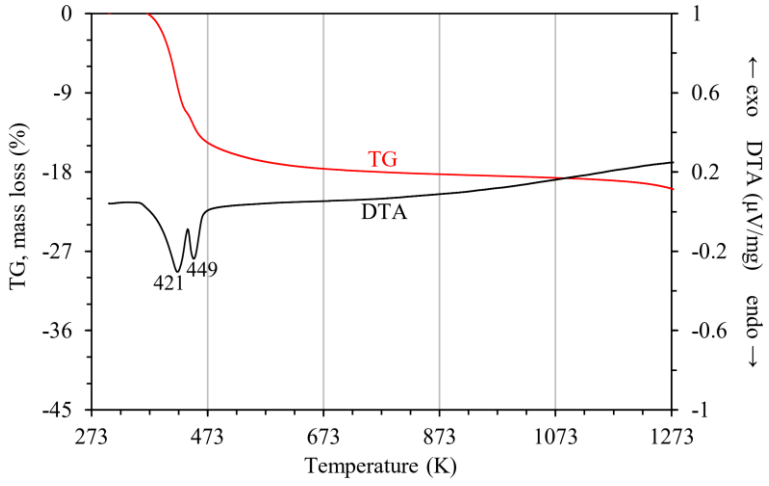


Figure 2. TG/DTA curves of $SrSO_4$-H_3BO_3 (S-B) mixture under air atmosphere

This was expected due to the positive Gibbs free energy values (Figure 3) of the SrB_2O_4 synthesis reaction (Equation (3)) at both 1073 K and 1273 K. The Gibbs free energy change calculations were performed using HSC Chemistry 10 (Metso Outotec) chemical reaction and equilibrium software. The XRD patterns of the S-B mixture heated at 1073 K and 1273 K (Figure 4) also substantiated that $SrSO_4$ and B_2O_3 did not react directly to form SrB_2O_4, probably due to the very high thermal stability of $SrSO_4$ (Equation (4), see also Figure 3) (Ostroff & Sanderson, 1959; Plewa et al., 1989; Lide, 2010).

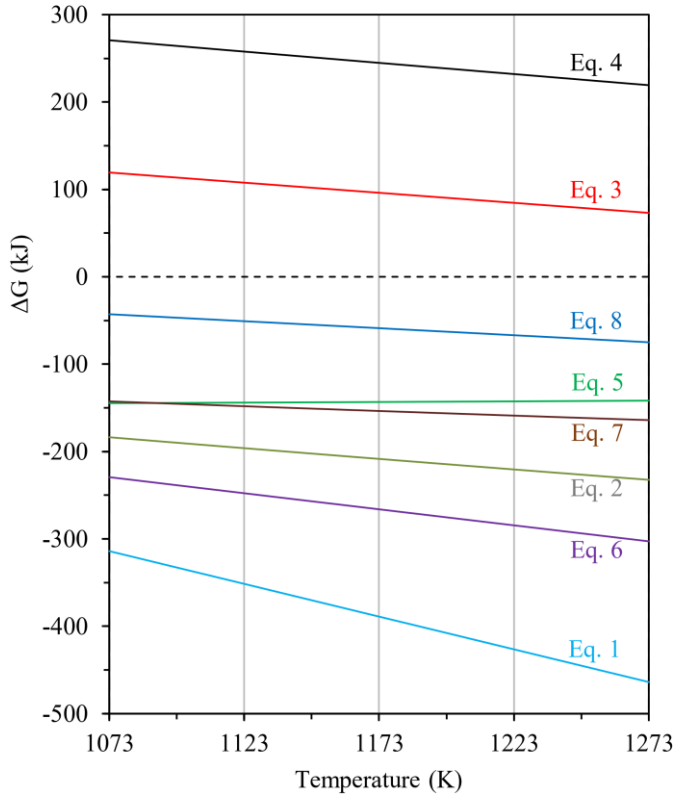


Figure 3. Variations of free energy values of the equations mentioned in the text with temperature

$$2H_3BO_3 \rightarrow B_2O_3 + 3H_2O \quad (2)$$

$$SrSO_4 + B_2O_3 \rightarrow SrB_2O_4 + SO_2 + 0.5O_2 \quad (3)$$

$$SrSO_4 \rightarrow SrO + SO_2 + 0.5O_2 \quad (4)$$

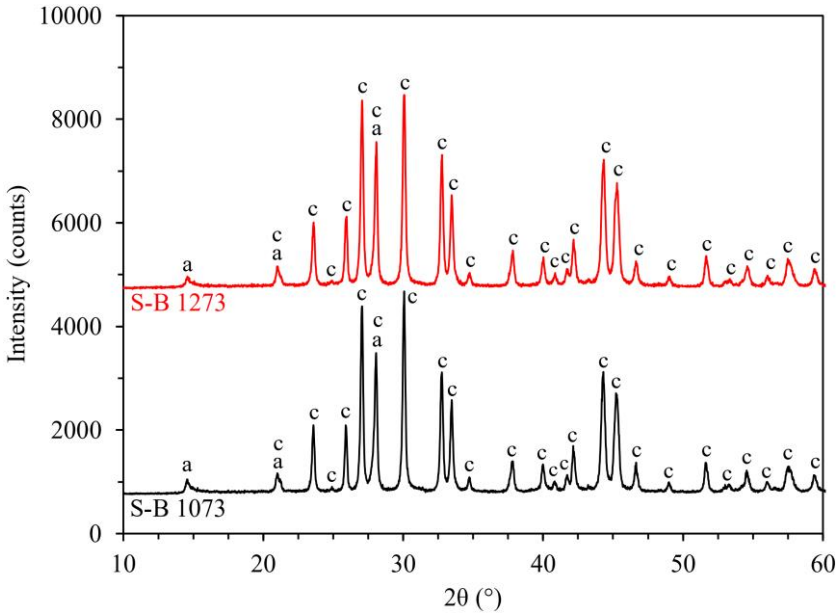


Figure 4. XRD patterns of $SrSO_4$-H_3BO_3 (S-B) mixtures heated in muffle furnace at 1073 K and 1273 K (a:H_3BO_3, c:$SrSO_4$)

As mentioned before, $SrSO_4$ has high thermal stability (thermally decomposes at 1647 K (Ostroff & Sanderson, 1959)) and in the presence of reducing agents, i.e. coal/coke (Chen & Zhu, 2000; Sezer et al., 2020), carbon monoxide (Plewa et al., 1989), methane (Ale Ebrahim & Jamshidi, 2009) or hydrogen (Hegedüs & Fukker, 1956; Habashi et al., 1976), it decomposes at lower temperatures by transforming to SrS. In the light of this information, before studying on $SrSO_4$-H_3BO_3-activated charcoal (S-B-C) mixture, the behaviour of $SrSO_4$-activated charcoal (S-C) mixture was investigated. The XRD patterns of the S-C mixtures heated in muffle furnace (Figure 5) indicated that $SrSO_4$ started to decompose by transforming to SrS by heating at 1073 K, above which the major mass loss for the S-C mixture initiated (see TG curve in Figure 6). This was expected due to the negative free energy values of Equation (1) at both 1073 K and 1273 K (see Figure 3). The XRD peak intensities of SrS (Figure 5), mainly observed at 2θ values of 25.63°, 29.68°, and 42.48° (match with JCPDS file no: 008-0489 for SrS), in the mixture heated at 1273 K indicated that higher amounts of SrS formed at higher heating temperature, as also observed in the related literature (Sonawane et al., 2000; Erdemoğlu, 2009; Setoudeh et al., 2011; Sezer et al., 2020). On the other hand, no XRD peaks belonging to other possible strontium-containing phases, for example, strontium oxide (SrO), were observed in Figure 5.

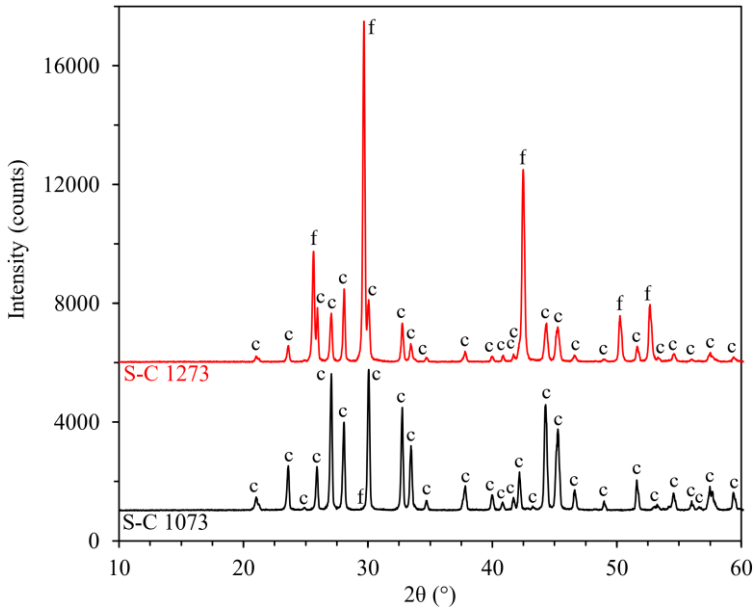


Figure 5. XRD patterns of $SrSO_4$-activated charcoal (S-C) mixtures heated in muffle furnace at 1073 K and 1273 K (c:$SrSO_4$, f:SrS)

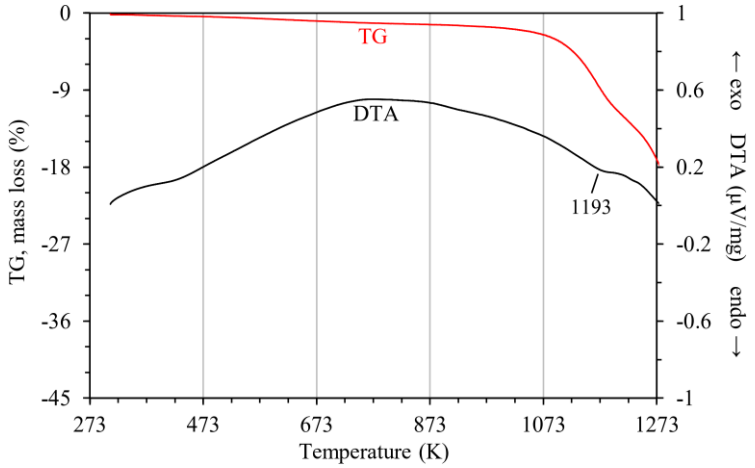


Figure 6. TG/DTA curves of $SrSO_4$-activated charcoal (S-C) mixture under inert atmosphere

Compared with the heat treatment performed at 1073 K in a muffle furnace containing a limited amount of oxygen, the heat treatment conducted at 1073 K in a tube furnace under a completely oxygen-free atmosphere resulted, as expected, in a higher amount of SrS in the heated mixture. Furthermore, after heat treatment at 1273 K in the tube furnace, the resulting material consisted entirely of the SrS phase (compare Figure 5 and Figure 7).

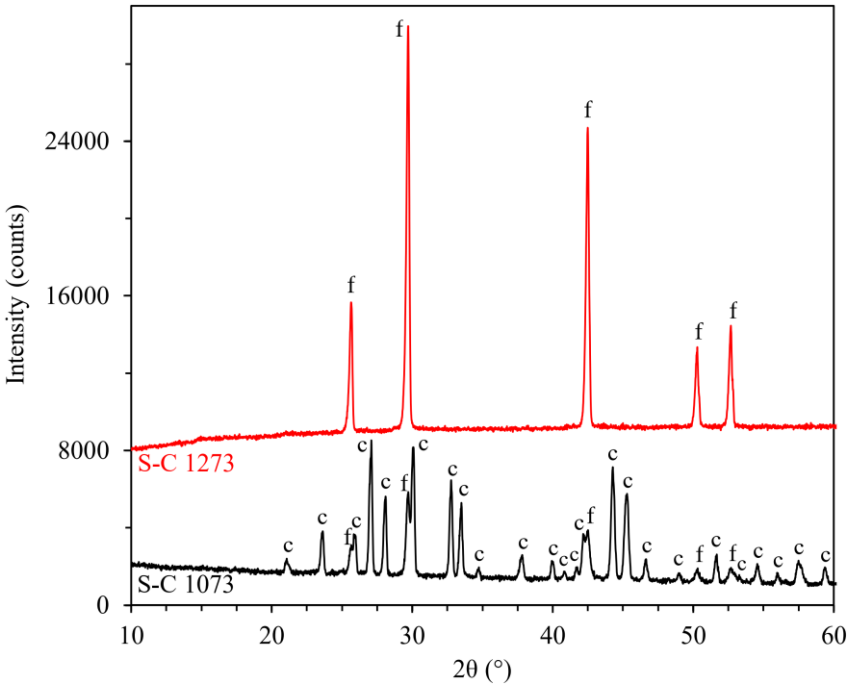


Figure 7. XRD patterns of $SrSO_4$-activated charcoal (S-C) mixtures heated in tube furnace at 1073 K and 1273 K (c:$SrSO_4$, f:SrS)

The high-temperature conversion of $SrSO_4$ to SrS is not a simple process and probably does not follow a single reaction. In addition to Equation (1), the reactions given in Equations (5) and (6) may also occur during heating in the reaction medium (Erdemoğlu, 2009; Meng et al., 2009; Setoudeh et al., 2011; Sezer et al., 2020). As seen in Figure 3, all three reactions are thermodynamically favourable between 1073 K and 1273 K. Furthermore, the presence of water vapour, originating from the decomposition of boric acid, in the reaction medium could transform $SrSO_4$ to SrS (Equation (7)) by the formation of reducing CO and H_2 gases according to Equation (8) (Parker, 1925), which is also possible (see Figure 3) between 1073 K and 1273 K.

$$SrSO_4 + 4CO \rightarrow SrS + 4CO_2 \quad (5)$$

$$SrSO_4 + 2C \rightarrow SrS + 2CO_2 \quad (6)$$

$$SrSO_4 + 4H_2 \rightarrow SrS + 4H_2O \quad (7)$$

$$C + H_2O \rightarrow CO + H_2 \quad (8)$$

Following the S-B and S-C mixtures, the behaviour of $SrSO_4$-H_3BO_3-activated charcoal (S-B-C) mixture during high-temperature heating was investigated. It was observed from Figure 8 that SrB_2O_4 did not form in the S-B-C mixture heated at 1073 K, where the XRD peaks of other strontium borate phases, i.e. SrB_6O_{10} and SrB_4O_7, were observed. This heating temperature (1073 K) coincides with the temperature of SrS formation, indicating that formation of strontium borate(s) is related with the formation of reactive SrS intermediate from $SrSO_4$ (compare the TG curves in Figure 6 and Figure 9). The XRD peaks observed at 2θ values of 14.71°, 27.09°, 28.11° and 30.95° (match with JCPDS file no: 015-0779 for SrB_2O_4) in the pattern of the S-B-C mixture heated at 1273 K proved that the SrB_2O_4 phase was formed. When the S-B-C mixture heated at 1273 K in tube furnace under inert atmosphere, SrB_2O_4 containing only SrS phase was formed (Figure 10). On the other hand, a comparison of Figure 8 and Figure 10 clearly indicates that effective reduction can be achieved during high-temperature heating not only in tube furnaces but also in muffle furnaces, commonly available in most laboratories, by employing carbon-based materials in conjunction with lidded crucibles, without the necessity of an inert gas flow.

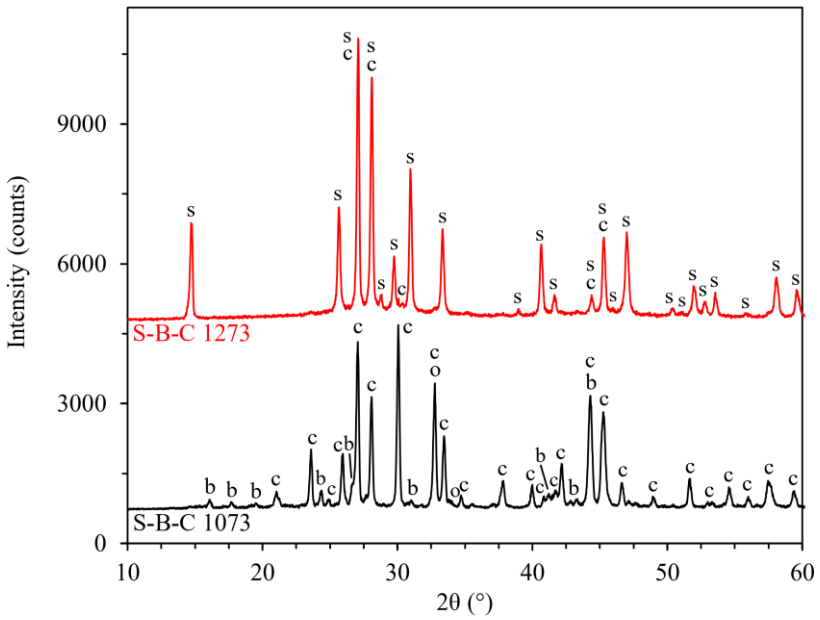


Figure 8. XRD patterns of $SrSO_4$-H_3BO_3-activated charcoal (S-B-C) mixtures heated in muffle furnace at 1073 K and 1273 K (b:SrB_6O_{10}, c:$SrSO_4$, o:SrB_4O_7, s:SrB_2O_4)

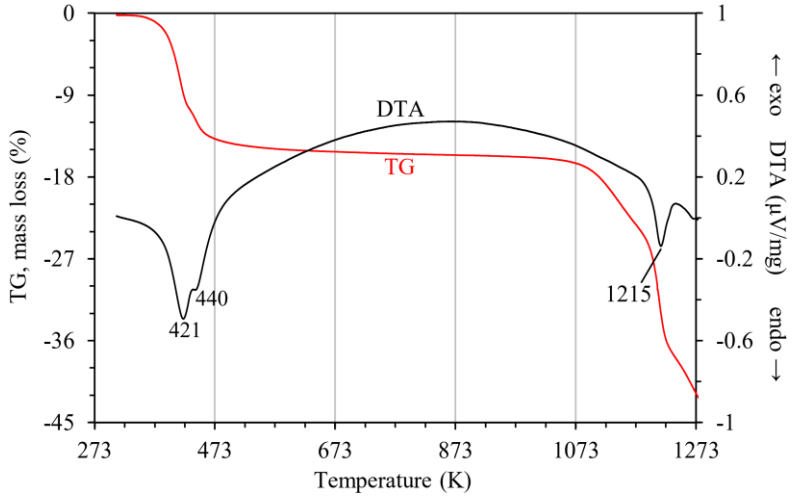


Figure 9. TG/DTA curves of $SrSO_4$-H_3BO_3-activated charcoal (S-B-C) mixture under inert atmosphere

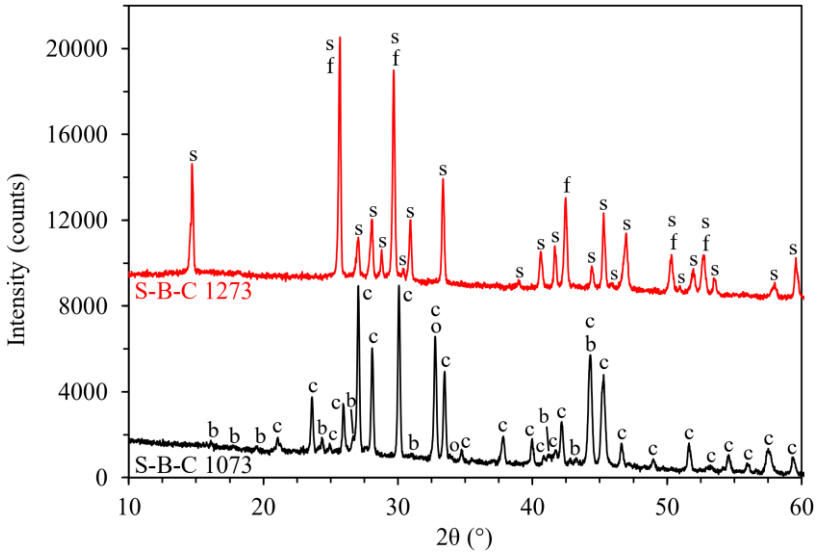


Figure 10. XRD patterns of $SrSO_4$-H_3BO_3-activated charcoal (S-B-C) mixtures heated in tube furnace at 1073 K and 1273 K (b:SrB_6O_{10}, c:$SrSO_4$, o:SrB_4O_7, s:SrB_2O_4, f:SrS)

As mentioned above, the formation of SrB_2O_4 was seemed to be dependent on the conversion of $SrSO_4$ to SrS intermediate during heating of the S-B-C mixture, in which the initial H_3BO_3 reactant is in the form of B_2O_3 intermediate between 1073 K and 1273 K. Taking this into account, the SS-BO mixture prepared from SrS and B_2O_3 were also heated separately in muffle and tube furnaces at 1273 K and the XRD patterns of the heated products were given in Figure 11. As shown in Figure 11, the SrB_2O_4 phase is predominantly formed after heat treatment in both types of furnaces. Because the binary SrS-B_2O_3 system, including the SS-BO mixture, has not yet been systematically investigated, further detailed investigations on its thermal behavior are recommended for future studies.

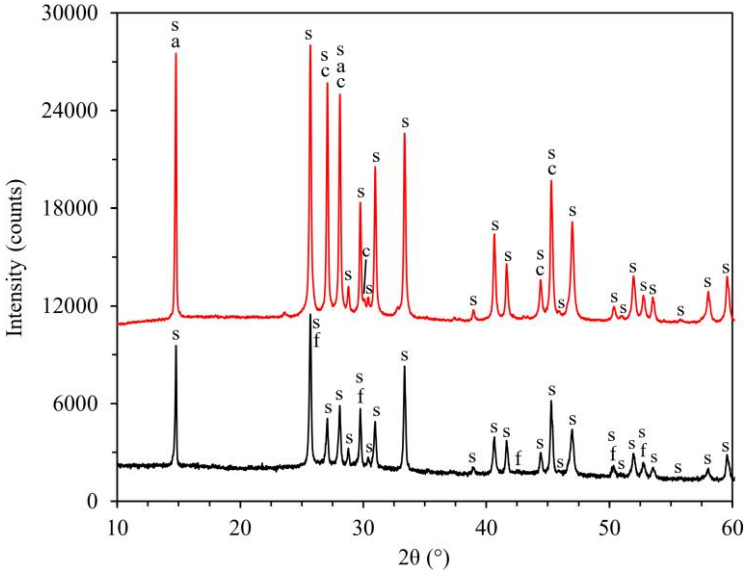


Figure 11. XRD patterns of SrS-B_2O_3 (SS-BO) mixtures heated in muffle (top) and tube (bottom) furnaces at 1273 K (a:H_3BO_3, c:$SrSO_4$, s:SrB_2O_4, f:SrS)

In addition to the XRD analyses, the formation of SrB_2O_4 was also substantiated by FTIR-ATR analyses (Figure 12). The absorption peaks observed at 633 cm^{-1}, 687 cm^{-1}, 730 cm^{-1}, 769 cm^{-1}, 1135 cm^{-1}, and 1419 cm^{-1}, all belong to the vibrations in infinite chains of trigonal borate groups (Rulmont & Almou, 1989) in SrB_2O_4. The obtained infrared spectra given in Figure 12 are well-matched with the spectra of SrB_2O_4 synthesized by Weir and Schroeder (1964) and Zhang et al. (2016) using reagent-grade $SrCO_3$ or SrO and H_3BO_3 compounds. On the other hand, the SEM images of the $SrSO_4$-H_3BO_3-activated charcoal (S-B-C) mixtures heated at 1273 both in muffle and tube furnaces (Figure 13) showed that both samples formed from heavily agglomerated/sintered irregularly shaped particles, as also observed in different literature studies (Wu et al., 2012; Zhao et al., 2012; Zhang et al., 2016).

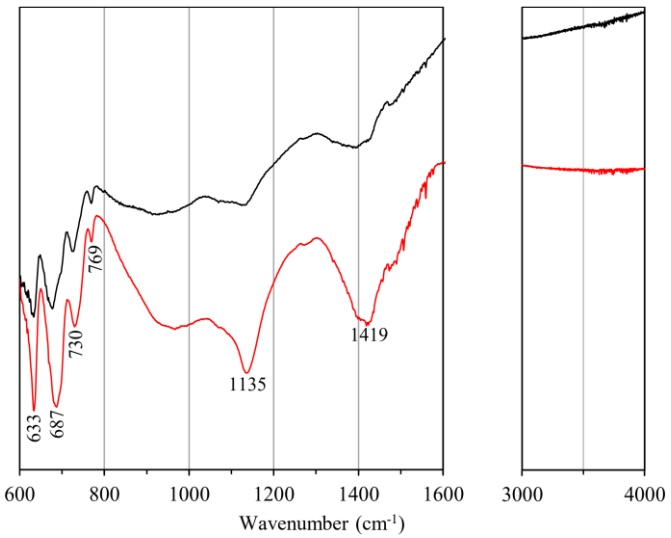


Figure 12. FTIR-ATR spectra of $SrSO_4$-H_3BO_3-activated charcoal (S-B-C) mixtures heated in muffle (red) and tube (black) furnaces at 1273 K

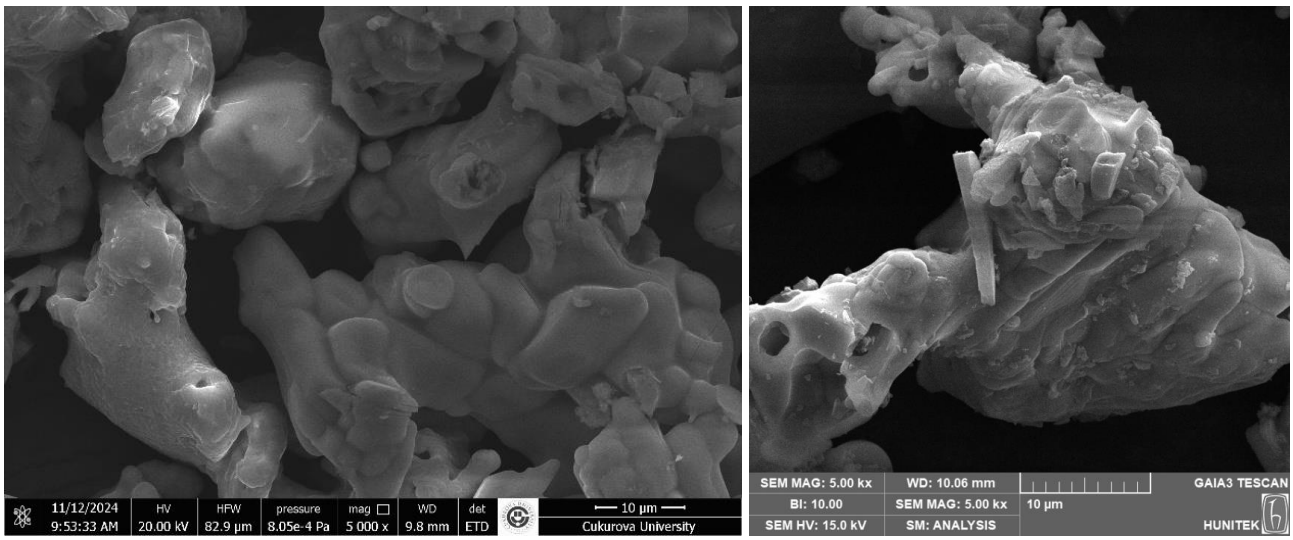


Figure 13. SEM images of $SrSO_4$-H_3BO_3-activated charcoal (S-B-C) mixtures heated in muffle (left) and tube (right) furnaces at 1273 K

The XRD patterns of celestine-activated charcoal (Cel-C) and celestine-H_3BO_3-activated charcoal (Cel-B-C) mixtures heated at 1273 K (Figure 14) in muffle furnace clearly indicated that celestine (natural $SrSO_4$), as the most common and the least expensive strontium source, may also be used for the preparation of SrB_2O_4 following optimization of the heating parameters.

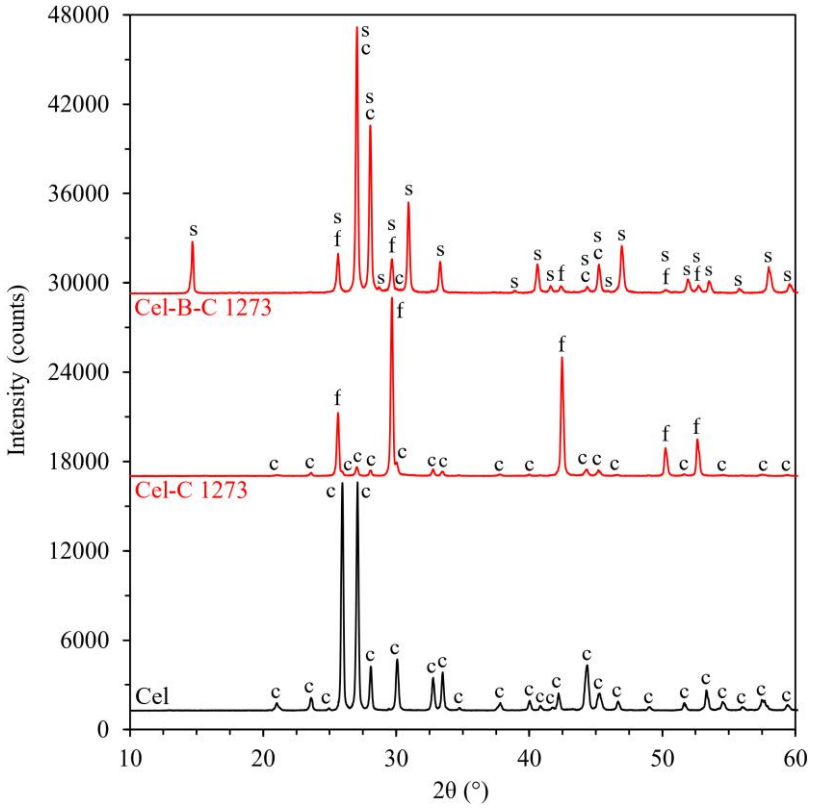


Figure 14. XRD patterns of celestine-activated charcoal (Cel-C) and celestine-H_3BO_3-activated charcoal (Cel-B-C) mixture heated at 1273 K in muffle furnace, together with celestine (c:$SrSO_4$, f:SrS, s:SrB_2O_4)

4. Conclusions

This study demonstrated that SrB_2O_4 can be prepared by interacting $SrSO_4$, either in reagent-grade or natural form, with H_3BO_3 at an $SrSO_4$:H_3BO_3 molar ratio of 1:2 in the presence of activated charcoal at 1273 K. The positive results of this study may create a different usage area for the highly abundant natural sources (borates/boric acid (Eti Maden, 2021) and celestine (Ermiş, 2011)) of Türkiye.

The promising results obtained in this study regarding the preparation of SrB_2O_4 also necessitate further investigation into the applicability of the high-temperature solid-state synthesis method employed here to the preparation of other strontium borates, e.g., SrB_4O_7 or $Sr_2B_2O_5$. In addition, the high-temperature solid-state synthesis of other alkaline earth metal (i.e., calcium) borate compounds from their naturally occurring sulfates, which yield more reactive sulfides in the presence of a reductant (carbon, methane, hydrogen etc.), should also be investigated in the future with the procedure used in this study.

Acknowledgement

The authors wish to acknowledge Fatih Çavuşlu (Adana Alparslan Türkeş Science and Technology Univ.), Sezgin Özkasapoğlu and Onur Berk Kutluata (both from Turkish Energy, Nuclear and Mineral Research Agency), and Hüseyin Evren Çubukçu (Hacettepe Univ.) for their help during experimental studies. The authors also wish to acknowledge Metso Outotec for the trial license of HSC Chemistry 10 software.

Author contribution

İ.E.: Investigation & writing. A.E.: Investigation, resources & writing. A.Ü.: Investigation & writing. R.S.: Investigation, resources & writing. A.O.: Conceptualization, methodology, investigation, resources & writing.

Declaration of ethical code

The authors of this article declare that the materials and methods used in this study do not require ethics committee approval and/or legal-special permission.

Conflicts of interest

The authors declare that there is no conflict of interest.

References

Abdel Halim, K. S., Ibrahim, S. S., & El-Barawy, K. A. (2009). Isothermal reduction behaviour of celestite concentrate by solid carbon. *Mineral Processing and Extractive Metallurgy*, *118*(4), 222-226. https://doi.org/10.1179/174328509X455322

Aghili, S., Panjepour, M., & Meratian, M. (2018). Kinetic analysis of formation of boron trioxide from thermal decomposition of boric acid under non-isothermal conditions. *Journal of Thermal Analysis and Calorimetry*, *131*, 2443-2455. https://doi.org/10.1007/s10973-017-6740-3

Ale Ebrahim, H., & Jamshidi, E. (2009). Kinetic study of celestite reduction by methane. *Mineral Processing and Extractive Metallurgy*, *Section C, 118*(4), 194-200. https://doi.org/10.1179/174328509X408289

Berezovskaya, I. V., Efryushina, N. P., Voloshinovskii, A. S., Stryganyuk, G. B., Pir, P. V., & Dotsenko, V. P. (2007). Luminescence and thermoluminescence of alkaline earth metaborates. *Radiation Measurements*, *42*(4-5), 878-881. https://doi.org/10.1016/j.radmeas.2007.02.029

Chen, W., & Zhu, Y. (2000). Preparation of strontium carbonate from celestite. *Mineral Processing and Extractive Metallurgy*, *109*(1), 1-5. https://doi.org/10.1179/mpm.2000.109.1.1

Erdemoğlu, M. (2009). Carbothermic reduction of mechanically activated celestite. *International Journal of Mineral Processing*, *92*(3-4), 144-152. https://doi.org/10.1016/j.minpro.2009.03.006

Ermiş, İ. U. (2011). *Production of Ammonium Sulfate and Strontium Carbonate via Leaching Methods from Strontium Sulfate Concentrate* [PhD Thesis, Selçuk University, Konya, Türkiye (in Turkish)].

Eti Maden. (2021). *Boron Sector Report*. Eti Mine Works. https://www.etimaden.gov.tr/storage/2021/Bor_Sektor_Raporu_2020.pdf (in Turkish).

Fujimoto, Y., Yanagida, T., Yokota, Y., Kawaguchi, N., Fukuda, K., Totsuka, D., Watanabe, K., Yamazaki, A., & Yoshikawa, A. (2011). Growth and characterization of strontium metaborate scintillators. *Optical Materials*, *34*(2), 444-447. https://doi.org/10.1016/j.optmat.2011.04.016

Gawande, A. B., Ingle, J. T., Sonekar, R. P., & Omanwar, S. K. (2014). Photoluminescence in Pb^{2+} activated SrB_4O_7 and SrB_2O_4 phosphors. *Journal of Luminescence*, *149*, 236-239. https://doi.org/10.1016/j.jlumin.2014.01.007

Griffiths, J. (1992). Celestite & Strontium chemical trade-The Mexican wave. *Industrial Minerals*, October, 21-33.

Habashi, F., Mikhail, S. A., & Van, K. V. (1976). Reduction of sulfates by hydrogen. *Canadian Journal of Chemistry*, *54*, 3646-3650. https://doi.org/10.1139/v76-524

Hatakeyama, T., & Liu, Z. (1998). *Handbook of Thermal Analysis*. John Wiley & Sons Ltd.

Hegedüs, von A. J., & Fukker, K. (1956). Thermoanalytischer beitrag zur zersetzung und reduktion der sulfate. *I. Zeitschrift für Anorganische und Allgemeine Chemie*, *284*(1-3), 20-30. https://doi.org/10.1002/zaac.19562840104

Hong, W. (1993). Celestite & Strontianite-Review of ore processing & exploitation. *Industrial Minerals*, June, 55-59.

IMA. (2022). International Mineralogical Association (IMA)-Commission on New Minerals, Nomenclature and Classification (CNMNC), The New IMA List of Minerals-A Work in Progress-Updated.

Kauffman, A. J. Jr., & Dilling, E. D. (1950). Differential thermal curves of certain hydrous and anhydrous minerals, with a desription of the apparatus used. *Economic Geology*, *45*(3), 222-244. https://doi.org/10.2113/gsecongeo.45.3.222

Li, R., Bao, L., & Li, X. (2011). Synthesis, structural, optical and mechanical characterization of SrB_2O_4 nanorods. *CrystEngComm*, *13*(19), 5858-5862. https://doi.org/10.1039/c1ce05537b

Lide, D. R. (Editor) (2010). *CRC Handbook of Chemistry and Physics*. 90th Ed., CRC Press, Boca Raton, Florida, USA.

Liu, Z. H., & Huang, H. S. (2006). Synthesis and thermochemistry of $SrB_2O_4 \cdot 4H_2O$ and SrB_2O_4. Thermochimica Acta, 448(1), 59-62. https://doi.org/10.1016/j.tca.2006.05.018

Meng, J., Liu, G., Zhao, H., Wang, L., & Yu, J. (2009). Mechanism study on carbon reducing reaction in the preparation process of strontium carbonate ($SrCO_3$). *Asia-Pacific Journal of Chemical Engineering*, *4*(5), 586-589. https://doi.org/10.1002/apj.291

Ohtsu, K., Yoshida, H., & Akamatsu, N. (1994). *Strontium borate pigment composition, method of making same, and processes for imparting anti-corrosive, anti-bacterial and/or anti-fungal, and non-flammable properties to materials by using same*. European Patent, EP0648818A1.

Onodera, A., Liu, X., Kyokane, D., Kura, K., & Machida, K. (1999). Pressure-induced amorphization of SrB_2O_4. *Journal of Physics and Chemistry of Solids*, *60*(10), 1737-1743. https://doi.org/10.1016/S0022-3697(99)00024-4

Ostroff, A. G., & Sanderson, R. T. (1959). Thermal stability of some metal sulphates. *Journal of Inorganic and Nuclear Chemistry*, *9*(1), 45-50. https://doi.org/10.1016/0022-1902(59)80009-9

Pan, X. M., Wang, C., & Jin, Z. P. (2004). Assessment of the thermodynamics and phase diagram of the SrO-B_2O_3 system. *International Journal of Materials Research*, *95*(1), 40-44. https://doi.org/10.3139/ijmr-2004-0008

Parker, A. (1925). The manufacture of blue water gas. *Nature*, *115*, 501-502. https://doi.org/10.1038/115501a0

Pekgözlü, İ., & Karabulut, H. (2009). Synthesis and photoluminescence of Pb^{2+} doped SrB_2O_4. *Inorganic Materials*, *45*, 61-64. https://doi.org/10.1134/S0020168509010105

Plewa, J., Steindor, J., Nowakowski, J., & Fitzner, K. (1989). Kinetics of $SrSO_4$ reduction with CO. *Thermochimica Acta*, *138*(1), 55-66. https://doi.org/10.1016/0040-6031(89)87241-7

Rulmont, A., & Almou, M. (1989). Vibrational spectra of metaborates with infinite chain structure: $LiBO_2$, CaB_2O_4, SrB_2O_4. *Spectrochimica Acta Part A: Molecular Spectroscopy*, *45*(5), 603-610. https://doi.org/10.1016/0584-8539(89)80013-3

Runowski, M., Woźny, P., Lavín, V., & Lis, S. (2018). Optical pressure nano-sensor based on lanthanide doped SrB_2O_4:Sm^{2+} luminescence - Novel high-pressure nanomanometer. *Sensors and Actuators B: Chemical*, *273*, 585-591. https://doi.org/10.1016/j.snb.2018.06.089

Setoudeh, N., Zamani, M. A. A., & Welham, N. J. (2011). Carbothermic reduction of mechanically activated mixtures of celestite and carbon. World Academy of Science, Engineering and Technology, *International Journal of Materials and Metallurgical Engineering*, *5*(2), 159-162. https://doi.org/10.5281/zenodo.1077183

Sevim, F., Demir, F., Bilen, M., & Okur, H. (2006). Kinetic analysis of thermal decomposition of boric acid from thermogravimetric data. *Korean Journal of Chemical Engineering*, *23*(5), 736-740. https://doi.org/10.1007/BF02705920

Sezer, R., Bilen, A., Hızlı, G., Ertürk, S., & Arslan, C. (2020). Effects of furnace slope and rotational speed on the carbothermic reduction of celestite in a laboratory-scale rotary kiln furnace. *Mining, Metallurgy & Exploration*, *37*(4), 1273-1278. https://doi.org/10.1007/s42461-020-00223-8

Sonawane, R. S., Apte, S. K., Kale, B. B., & Dongare, M. K. (2000). Effect of a catalyst on the kinetics of reduction of celestite ($SrSO_4$) by active charcoal. *Metallurgical and Materials Transactions B*, *31*, 35-41. https://doi.org/10.1007/s11663-000-0128-6

Üçyıldız, A. (2008). Solid-State High Temperature Synthesis and Characterization of $MgO{\cdot}xB_2O_3$ Compounds. [MSc Thesis, Hacettepe University, Ankara, Türkiye (in Turkish)].

Weir, C. E., & Schroeder, R. A. (1964). Infrared spectra of the crystalline inorganic borates. *Journal of Research of the National Bureau of Standards*. *Section A*, *Physics and Chemistry*, *68*(5), 465-487. https://doi.org/10.6028/jres.068A.045

Wu, Z. C., Wan, P., Liu, J., Li, C., Zhou, W. H., & Kuang, S. P. (2012). Improved photoluminescence properties of a new green $SrB_2O_4:Tb^{3+}$ phosphor by charge compensation. *Materials Research Bulletin*, *47*(11), 3413-3416. https://doi.org/10.1016/j.materresbull.2012.07.013

Zhang, J., Han, B., Zhang, Y., & Lv, Q. (2016). Luminescence properties of Ce^{3+} in strontium borate SrB_2O_4. *Journal of Materials Science: Materials in Electronics*, *27*, 3906-3910. https://doi.org/10.1007/s10854-015-4241-3

Zhao, L. S., Liu, J., Wu, Z. C., & Kuang, S. P. (2012). Optimized photoluminescence of $SrB_2O_4:Eu^{3+}$ red-emitting phosphor by charge compensation. *Spectrochimica Acta Part A: Molecular and Biomolecular Spectroscopy*, *87*, 228-231. https://doi.org/10.1016/j.saa.2011.11.043

Zheng, J., Ying, L., Cheng, Q., Guo, Z., Cai, L., Lu, Y., & Chen, C. (2015). Blue-emitting $SrB_2O_4:Eu^{2+}$ phosphor with high color purity for near-UV white light-emitting diodes. *Materials Research Bulletin*, *64*, 51-54. https://doi.org/10.1016/j.materresbull.2014.12.051

Zheng, T., Runowski, M., Woźny, P., & Lis, S. (2020). Influence of matrix on the luminescence properties of Eu^{2+}/Eu^{3+} doped strontium borates: SrB_4O_7, SrB_2O_4 and $Sr_3(BO_3)_2$, exhibiting multicolor tunable emission. *Journal of Alloys and Compounds*, *822*, 153511. https://doi.org/10.1016/j.jallcom.2019.153511